



Brief communication: Analysis of organic matter in surface snow by PTR-MS – implications for dry deposition dynamics in the Alps

Dušan Materić¹, Elke Ludewig², Kangming Xu¹, Thomas Röckmann¹, Rupert Holzinger¹

¹Institute for Marine and Atmospheric Research Utrecht, Utrecht University, Princetonplein 5, 3584CC Utrecht, The Netherlands

²ZAMG - Zentralanstalt für Meteorologie und Geodynamik, Sonnblick Observatory, A-5020 Salzburg, Freisaalweg 16, AUSTRIA

Correspondence to: Dušan Materić (dusan.materic@gmail.com)

Abstract. The exchange of organic matter (OM) between the atmosphere and snow is poorly understood due to the complex nature of OM and the convoluted processes of deposition, re-volatilisation, chemical, and biological processing. OM that is finally retained in glaciers potentially holds a valuable historical record of past atmospheric conditions; however, our understanding of the processes involved is insufficient to translate the measurements into an interpretation of the past atmosphere. This study examines the dynamic processes of post-precipitation OM change at the alpine snow surface with the goal to interpret the processes involved in surface snow OM.

1 Introduction

Organic matter (OM) in the cryosphere originates from different sources (e.g. oxidation products of anthropogenic, biogenic, and biomass burning VOCs), is transported from short and long distances and is deposited via dry or wet deposition (Antony et al., 2014). From the moment of the emission, OM undergoes atmospheric chemistry processes, which profoundly alter the chemical composition of OM, resulting in numerous chemical species that are finally deposited on the snow/ice surface (Legrand et al., 2013; Müller-Tautges et al., 2016). Fingerprints of OM stored in the snow and ice therefore potentially hold a rich historical record of atmospheric chemistry processes and the transport pathways in the atmosphere (Fu et al., 2016; Giorio et al., 2018; Grannas et al., 2006; Pokhrel et al., 2016). The vast diversity of OM, which is found in snow and ice samples, is impossible to characterise by one single method. The most used methods so far in snow/ice OM research are based on gas chromatography (GC) and liquid chromatography mass spectrometry (LC-MS) (Giorio et al., 2018; Gröllert et al., 1997). Novel high-resolution mass-spectrometry-based analytical methods, such as Fourier-transform ion cyclotron resonance mass spectrometry (FT-ICR-MS), Orbitrap mass spectrometry, and Thermal Desorption – Proton Transfer Reaction – Mass Spectrometry (TD-PTR-MS), have recently been developed and can be used to characterise OM in the cryosphere with high mass resolution (Hawkes et al., 2016; Kujawinski et al., 2002; Marsh et al., 2013; Materić et al., 2017).



35 Therefore, numerous new proxies are now potentially available to interpret the rich composition of OM
in the cryosphere.

Reconstructing past atmospheric conditions from measurements of OM in the cryosphere is analytically
challenging because of (1) low concentrations of target organics in the sample, and (2) chemical
changes that (might) happen after OM deposition. A recently developed method using Thermal
Desorption – Proton Transfer Reaction – Mass Spectrometry (TD-PTR-MS) has partly solved the first
40 issue enabling the detection of low molecular weight OM ranging from 28 to 500 amu (Materić et al.,
2017). However, chemical changes (e.g. photochemical, biological etc.) and re-emission from the
snow/ice surface still remain challenging to quantify, especially in the context of the diversity of OM
species, both high and low molecular weight OM.

The low molecular weight fraction represents an important part of OM in the cryosphere and the group
45 includes volatile and semi-volatile organic compounds (VOC, sVOC) that deposit directly from the gas
phase or as part of secondary organic aerosols (SOA). Low molecular weight OM has been extensively
studied in atmospheric context by real-time or off-line PTR-MS techniques (Gkatzelis et al., 2018;
Holzinger et al., 2010a, 2013; Materić et al., 2015; Timkovsky et al., 2015), however, not so in the
context of deposited (e.g. dissolved) OM in the cryosphere. In this work, we applied a novel TD-PTR-
50 MS method to measure concentrations of OM present in Alpine snow. The first application of this new
technique is investigation of snow-atmosphere interaction of OM during a dry weather period.

2 Material and methods

2.1 Sampling site

55 The snow samples were taken at 3.106 m altitude at Mt. Hoher Sonnblick, Austria, close to the research
station Sonnblick Observatory. The sample site was next to the southern precipitation-measuring
platform, which is about 50 m southeast of the observatory. The sampling location was carefully chosen
to be least affected by potential contamination coming from the observatory. Average temperature of
the site is about 1.1°C in summer and -12.2°C in winter considering the meteorological data being
gathered since 1886.

60 The sample period spans the days from March 20th to April 1st of 2017. During this time period the
Sonnblick Observatory experienced an average day length of 12.5 hours, and an average temperature of
-4°C, 78% relative humidity, an average wind speed of 7.3 m s⁻¹ and pressure of 696 hPa. There was no
significant precipitation observed but these days were mostly foggy in the morning with the exception
of March 27th and 28th 2017, which were nearly clear-sky days, followed by less cloudy days till April
65 1st 2017. The measured air temperatures (2 m above the surface) on the site were below zero for all the
time, with exception of 3 brief instances where the temperature was recorded 0.1°C for 10 minutes (Fig.
1a). However, hourly temperature averages for these events were also < 0°C. If we use a Positive
Degree Day model (PDD) to assess the melting possibility of those single 10 minutes periods, we
calculated the depth of the melt water 1.4-5.5 µm (using the snow melt factor 2-8 mm °C⁻¹ day⁻¹) (Singh
70 et al., 2000). Thus, we conclude that no significant melting and runoff happened for the entire sampling
period.



More information on the meteorological conditions can be found in Fig. 1 and Fig. A1.

2.2 Sampling

75 Snow samples were taken from the surface snow (<2 cm) scooping the snow directly into clean 50 mL polypropylene vials. We also took field blanks (ultrapure water) to assure that our blanks were exposed to the same impurities as the snow samples. The samples were stored in a freezer at -20°C until the end of the sampling campaign and then shipped on dry ice to the analysis lab, where they were kept frozen until the analysis.

80 2.3 Analysis

Prior to the analysis the samples (and blanks) were melted and filtered through a 0.2 µm PTFE filter. We loaded 1 mL of each sample into clean 10 mL glass vials that had been prebaked at 250°C overnight. The samples (in triplicates) together with the field blanks, were dehydrated using a low-pressure evaporation/sublimation system and analysed by TD-PTR-MS (PTR-TOF 8000, IONICON
85 Analytik), following the method described before (Materić et al., 2017). The thermal desorption procedure was optimized for snow-sample analysis and has the following temperature sequence: (1) 1.5 min incubation at 35 °C, (2) ramp to 250 °C at a rate of 40 °C min⁻¹, (3) 5 minutes at 250 °C, and (4) cooling down to <35 °C. The method is fast (<15 min per run), sensitive (e.g. LoD <0.17 ng mL⁻¹ for pinonic acid, LoD<0.26 ng mL⁻¹ for levoglucosan), requires a small sample size (<2 mL of water), and
90 it provides reasonably high mass resolution data (>4500, FWHM).
For the data analysis, we used the custom made software package PTRwid for peak integration and identification, and R scripts for statistical analyses (linear regression, fitting etc.) (Holzinger, 2015). We used 3σ of the field blanks for estimating the limit of the detection (LoD), so only ions that are above this value were taken into account for the scientific interpretation (Armbruster and Pry, 2008). We
95 evaluated the impurities in the field blanks by comparing them with the system blanks (clean vials) and discovered that the average impurity level of a field blank was reasonably low (7.0 ng mL⁻¹), which mostly (60 %) originated from the ion m/z 81.035 (C₃H₄OH⁺). The impurities here might originate from the polypropylene vials we used, however, the levels are much lower compared to the methods used for measuring total and dissolved OM (Giorio et al., 2018). The impurities were taken into account by
100 means of field blank subtraction and LoD filtering (Materić et al., 2017).
From the mass spectra, identified peaks were integrated over 8 minutes starting when the temperature in the TD system reached 50°C. Extracted peaks were quantified by PTRwid and the concentration was expressed in ng mL⁻¹ of sample. We calculated the molar concentration of C, H, O and N for each sample, from which atomic ratios (O/C, H/C, N/C), mean carbon number (nC), and mean carbon
105 oxidation state (OSC) are calculated as described earlier (Holzinger et al., 2013; Materić et al., 2017).
For the elemental composition calculation, we excluded ions m/z <100 as these are dominated by thermal dissociation products of non-volatile high molecular weight compounds. Taking into account these fragments of bigger molecules would substantially alter elemental composition and atomic ratios.



3 Results and Discussion

110 3.1 Total ion concentration and simple mass balance model

During our sampling period, the total concentration of organics increases in general over the time that the snow was exposed to the atmosphere (Fig. 2a). The concentration of organics in the snow surface reflects a dynamic balance between two opposing processes that work independently: deposition as source and loss. If we consider just dry deposition (it was a period without precipitation), the retained
115 (actual) concentration of the organics in the snow can be described as:

$$\frac{dm}{dt} = D - L, \quad (1)$$

where m is the concentration of organics remaining in the snow, D is the total dry deposition rate and L is the overall loss rate due to re-volatilisation, photochemical reactions, biological processes etc. As our samples generally show an increase in the ion concentrations (Fig. 2 and 3), the loss rate by re-
120 volatilisation, photochemical reaction and biological decay is lower than the total deposition rate ($D > L$). A negative mass balance, i.e. $D < L$, can happen, for example, in periods of extensive photochemical reactions together with snow exposure to an air mass with a low concentration of OM.

Our total concentration data (as well as many individual ion groups, see below) indicate a relaxation towards a source-sink equilibrium. Mathematically, the simplest model that has these characteristics is a
125 system with quasi-constant deposition rate D (i.e. changes in deposition are much slower than changes in the loss rate) and a first order loss rate ($L = km$ in equation 1), which can be integrated to yield

$$m = m_0 e^{-kt} + \frac{D}{k} (1 - e^{-kt}), \quad (2)$$

where m_0 is the initial concentration of m , k is the first order loss rate coefficient and t is time. In our experiment, we measured m with a time step t of three days and consider m_0 as our measurement of the
130 fresh snow in the beginning of the analysis period. Eq. 2 can then be fit to the data and the best fit for the total concentration of semi-volatile organic traces ($R^2 > 0.98987$ and $rRMSE < 3.5\%$) was found for $k = 0.31 \text{ day}^{-1}$ and $D = 206 \text{ ng mL}^{-1} \text{ day}^{-1}$. When the fit is applied to the mass of carbon in the detected organics the best fit values for the two parameters are $k = 0.30 \text{ day}^{-1}$ and $D = 114 \text{ ng mL}^{-1} \text{ C day}^{-1}$ respectively). Considering reported average organic aerosol (OA) concentration we assume the winter
135 air concentration (C) to be at most $2 \mu\text{g C m}^{-3}$ (Guillaume et al., 2008; Holzinger et al., 2010b; Strader et al., 1999). Further taking an average sampling depth of 2 cm and a snow density of 250 mg mL^{-1} we calculated a deposition velocity of 0.33 cm s^{-1} according to equation (3):

$$v = \frac{D}{C \times A} \quad (3)$$

140 where D is the measured deposition rate, C is concentration ($2 \mu\text{g C m}^{-3}$) and A is the area that was typically sampled (combining sampling depth and snow density relates 1 mL of sample to an area of 2 cm^2). Assuming slightly higher ($3 \mu\text{g C m}^{-3}$) or lower ($1 \mu\text{g C m}^{-3}$) organic aerosol concentration in air, and sampling variation between 1.5-2 cm depth we calculated positive error of factor of 2 and negative
145 error of factor of 2^{-1} . Thus, deposition velocity for organic aerosols of $0.17\text{-}0.66 \text{ cm s}^{-1}$ would be



required to be consistent with the observations. However, the deposition velocities for organic aerosol were previously estimated to be 0.034 ± 0.014 and 0.021 ± 0.005 cm s^{-1} for particles in 0.15–30 and 0.5–1.0 μm size ranges (Duan et al., 1988; Gallagher et al., 2002). The required deposition velocities are approximately an order of magnitude higher than the previously reported estimates even if we use the upper limit of expected organic aerosol concentration ($2 \mu\text{g C m}^{-3}$). Therefore, we conclude that the dominating contribution to OM in the snow is from gas phase sVOCs. As direct measurements of bulk sVOCs do not exist, we estimated the required average loads of sVOCs in the air passing the sampling location to explain the observations. Using the deposition rate calculated from our measurements (Eq. 2), the concentration-weighted average molecular mass of measured compounds, and deposition velocities of 1 cm s^{-1} (assuming that sVOC deposition velocities are similar to the one of formic acid) (Nguyen et al., 2015), we calculated an average gas phase sVOC burden of 883 ng m^{-3} of air which is equivalent to 247 ppt. Assuming slightly higher or lower deposition velocities ($\pm 0.2 \text{ cm s}^{-1}$) yield errors of +221 and -148 ng m^{-3} , or +62 and -41 ppt. Our calculated value of average sVOC concentration agrees with previous estimates of $0.6 \mu\text{g m}^{-3}$ (Zhao et al., 2014). Thus, our data suggest that dynamic processes of DOM on the surface snow are dominated by deposition and re-volatilisation of gas phase sVOCs. This has important implications for our understanding of the snow surface processes. Our analysis suggests that air masses with different sVOC composition can leave different OM fingerprints in the snow (discussed in the sections below).

The D/k ratio quantifies the equilibrium point (asymptote) for the model described in Eq. (2). This represents a point at which the equilibrium is established between deposition and losses. The derived time constant for loss of about 3 days implies that 90% equilibrium is established for the total ion concentration in only 6 days. This value, however, represents an average equilibrium time for total measured DOM, and it is reasonable to assume that this equilibration timescale differs between different compounds. In particular, it is estimated to be established much faster for the gas-phase sVOCs compared to SOA.

Similar mass balance calculations will be carried out in the following section for individual ion groups.

3.2 Grouping of ions with similar time evolution

In the data analysis of TD-PTR-MS spectra, we found 270 organic ions above the detection limit present in the samples. Compounds that have the same origin (similar sources or atmospheric chemistry processes) should feature similar time evolution, if the lifetime is not so short that such a common time evolution is lost. Based on the pattern of concentration change over time (using Pearson correlation) we identified four groups of ions with similar time evolution (Fig. 3, Table A1). In the group 1, 2, 3 and 4 we assigned 25, 33, 9 and 21 ions respectively (88 ions in total 33%), and 175 ions did not fall in any of these groups. Ions which we did not assign to any group either showed different time evolution or had concentrations close to the detection limit causing poor correlation. In average, the total concentration levels of the ions within the four groups were 30, 56, 16, 57 ng mL^{-1} respectively, and 315 ng mL^{-1} for ions which did not fall in any of the described groups. Specific information can be found in the supplementary data.



185 In the first two groups (Fig. 3a and b), among the numerous ions we identified masses that we tentatively attribute to pinonic acid (m/z 115.07 fragment) and levoglucosan (e.g. m/z 85.03 and 97.03 fragments). Pinonic acid is an oxidation product of monoterpenes and the main source is expected to be emission from surrounding alpine conifer forests, thus group 1 ions indicate air masses that were originally rich in biogenic VOC, which have been processed during transport. Levoglucosan is a clear indicator of biomass burning and the most likely source during this period is domestic wood combustion. Therefore, we associate group 2 ions to the anthropogenic wood combustion sources and their products in the complex atmospheric processing.

190 The compounds that fall in group 3 show, after an initial increase in the concentration on 23/03/2017, a decreasing trend (Fig 3c, see also Table A1). The change in the concentration of the compounds constituting this group may point to a one-time significant pollution event which happened between 20th and 23rd of March. The total concentration of ions in this group was measured to be 34 ng mL^{-1} (8.2% of the total organics) on 23/03/2017. This deposition event could have come from a single source, however higher time resolution measurements are needed to further characterize the potential source.

195 As total concentration of ions in this group drops in 6 days below 20 ng mL^{-1} (3.1% of the total organics), this group is also an example how contaminated snow equilibrates with the cleaner atmosphere on similar timescales as we derived from the simple box model.

200 As for total concentration, most of the ions and ion groups show an increase in the ion concentrations throughout the sampling period. Group 4 (Fig. 3d, Table A1) represents the compound group for which the concentration seems steadily increasing towards an equilibrium. This indicates that the simple mass balance model may be applicable, i.e., the assumption of a (close to) constant deposition and first order loss rate. Therefore we applied the simple mass balance model (see 3.1.) also to the individual ions in group 4 to investigate whether individual organic compounds have different k values. This is expected due to the different chemical and physical properties (such as volatility, amenability to photolysis etc.) as well as different nutrition adequacy for potential biodegradation. For the sum of organic ions in the group 4 (Fig. 3d, Table A1), $k = 0.20 \text{ day}^{-1}$. Generally, the lower k value of this group compared to the total sVOC could be related to the fact that most of the ions here are heavier (thus, less volatile).

205 However, within this group k values of individual ions were found to be independent of the molecular weight, and also independent of the composition, i.e. O/C, H/C, OSC and nC ($R^2 < 0.12$). As the volatility of sVOC is expected to depend on molecular weight and functional groups (longer sVOC are in general less volatile, unless additional functional groups are involved), this suggests that volatility might not play the only role in the loss processes of this group.

210 A deviation in the general concentration trend of individual ions (from the expected growth, section 3.1) was observed on 29/03/2017, particularly in the groups 1 and 2 represented by pinonic acid and levoglucosan (Fig. 3a and b). Elevated levoglucosan and lower pinonic acid levels observed at 29th are temporally related to a change in wind direction. On the 29th, the air masses originate from the North-East direction, rather than North-West direction, seen for other samples (Fig 1c), so this event is attributed to the meteorological situation.

215 Presence of such distinctive patterns of concentration change over time, ion grouping, and their relation with the meteorological data indicate that meteorology and deposition of sVOCs after fresh precipitation strongly affect the organic composition in snow, which questions the most straightforward approach of interpreting of OM signals in terms of organic aerosol in the air.

225



3.2 Elemental composition

230 We further investigate the processing of OM in snow during the study period by calculating cumulative
metrics of the OM composition from the PTR-MS data, namely the elemental ratios O/C and H/C, the
number of carbon atoms per compound, nC, and the oxidative state OSC of the organic carbon, in order
to further characterize the processes behind the observed changes. The fresh snow sample (20/04/2017)
has the lowest total concentration of all measured organics, low OSC, the lowest O/C and N/C value,
235 and high H/C and nC value (Fig. 2), which all indicate ‘fresh’ OM in the air (Kroll et al., 2011), which
was captured in the snow.

An interesting signature in the metrics is observed on 29/03/2017 when the prevailing air flow regime
was interrupted (wind direction change, Fig. 1c). This sample showed the highest value of nC, the
lowest OSC, as well as elevated H/C and low O/C ratios (Fig. 2). This all indicates photochemically
240 younger (fresher) emissions of VOC and semi-volatiles, originating from air-masses rich in biomass
burning aerosols (Fig. 3b), which is in agreement with previous results linking low OSC and high nC to
biomass burning aerosols (Kroll et al., 2011). However, on the 29th we also observed lower total OM
concentration in the sample compared to the previous period which clearly indicates a net loss of OM.
Potential processes that could explain such loss of OM involve photolysis induced re-volatilisation, OM
runoff (e.g. snow melting), or oxidation. The photolysis induced volatilization should be higher for this
245 sample as the previous days (27th and 28th) had the highest global radiation values (33% higher the
average for the sampling period) and the longest sunshine duration (>12 hours) (Fig 1b and Fig. A1).
On the other hand, no significant temperature increase has been measured to support increased melting
and OM runoff. Loss by oxidation (referring to “dark” oxidation that is uncoupled from photooxidation)
is also unlikely as main process since the O/C ratio did not increase for 29th of March (Fig. 3c). Thus,
250 the most likely cause of the lower total OM concentration observed on march 29 is re-volatilization,
possibly enhanced by photolysis, which would indicate that the air contained a lower burden of SVOCs.
In addition, new OM material with different characteristics was deposited before that sample was
collected. Combining all metrics (Fig. 2) and meteorological data available (Fig. 1), we can conclude
that the air passing the site prior to 29/03/2017 was cleaner and photochemically younger, and
255 contained higher MW compounds that might have originated from anthropogenic emissions such as
biomass burning (high levels of levoglucosan, Fig. 3).

4 Conclusion

In this work, we analysed the concentrations of low molecular weight organic matter (20 – 500 amu) in
Alpine snow samples during a 12-day no-precipitation period, 20.03-01.04.2017. We noticed four
260 distinctive groups of ions with similar concentration trend over that time ($R^2 > 0.9$), suggesting common
sources, chemistry processes, or transport pathways. The largest two groups of ions came from (a)
surrounding forests (e.g. pinonic acid – associated with monoterpene oxidation) and (b) residential fires
(levoglucosan – common biomass burning marker). The snow sample taken on 29th of March showed a
change in the general concentration trend, consistent with a shift in wind direction, indicating different



265 air mass origin. This is also in agreement with a change in atomic ratio metrics (O/C, H/C, OSC and
nC), which also indicated that re-volatilization is the most important pathway of OM loss here,
suggesting that the advected air was cleaner during this period. Dry deposition can be approximated by
a mass balance model with a roughly constant deposition rate of $D = 206 \text{ ng mL}^{-1} \text{ day}^{-1}$ and a first order
loss rate constant $k = 0.31 \text{ day}^{-1}$. Calculated deposition velocities were inconsistent with the idea that
270 organic aerosols contribute the bulk of deposited OM, instead we suggest a dominant contribution of
gas-phase sVOC over the OA in the total bulk organic matter. This all indicates that, at least for this site
and location, snow-atmosphere DOM exchange processes are mostly driven by gas-phase sVOCs, for
which equilibration with air is fast. This has implications for the reconstruction of recent atmospheric
conditions by analysis of organics in the snow.

275 **Data availability**

Data are available via:

http://www.projects.science.uu.nl/atmosphereclimate/Data/Supplement_data_PTR-SNOW.xlsx

Author contribution

DM and RH designed the experiments and DM carried them out. LE provided the samples and
280 meteorological data. DM prepared the manuscript with contributions from all co-authors.

Competing interests

The authors declare that they have no conflict of interest.

Acknowledgements

Tis work is supported by Netherlands Earth System Science Centre (NESSC) research network and by
285 the Dutch NWO Earth and Life Science (ALW), project 824.14.002. We thank the operators at the
Sonnblick observatory for taking the samples.

References

Antony, R., Grannas, A. M., Willoughby, A. S., Sleighter, R. L., Thamban, M. and Hatcher, P. G.:
290 Origin and sources of dissolved organic matter in snow on the East Antarctic ice sheet, Environ. Sci.
Technol., 48(11), 6151–6159, doi:10.1021/es405246a, 2014.



- Armbruster, D. A. and Pry, T.: Limit of Blank, Limit of Detection and Limit of Quantitation, *Clin. Biochem. Rev.*, 29(Suppl 1), S49–S52, 2008.
- 295 Duan, B., Fairall, C. W. and Thomson, D. W.: Eddy Correlation Measurements of the Dry Deposition of Particles in Wintertime, *J. Appl. Meteorol.*, 27(5), 642–652, doi:10.1175/1520-0450(1988)027<0642:ECMOTD>2.0.CO;2, 1988.
- Fu, P., Kawamura, K., Seki, O., Izawa, Y., Shiraiwa, T. and Ashworth, K.: Historical Trends of Biogenic SOA Tracers in an Ice Core from Kamchatka Peninsula, *Environ. Sci. Technol. Lett.*, 3(10), 351–358, doi:10.1021/acs.estlett.6b00275, 2016.
- 300 Gallagher, M. W., Nemitz, E., Dorsey, J. R., Fowler, D., Sutton, M. A., Flynn, M. and Duyzer, J.: Measurements and parameterizations of small aerosol deposition velocities to grassland, arable crops, and forest: Influence of surface roughness length on deposition, *J. Geophys. Res. Atmospheres*, 107(D12), AAC 8-1-AAC 8-10, doi:10.1029/2001JD000817, 2002.
- 305 Giorio, C., Kehrwald, N., Barbante, C., Kalberer, M., King, A. C. F., Thomas, E. R., Wolff, E. W. and Zennaro, P.: Prospects for reconstructing paleoenvironmental conditions from organic compounds in polar snow and ice, *Quat. Sci. Rev.*, 183, 1–22, doi:10.1016/j.quascirev.2018.01.007, 2018.
- Gkatzelis, G. I., Tillmann, R., Hohaus, T., Müller, M., Eichler, P., Xu, K.-M., Schlag, P., Schmitt, S. H., Wegener, R., Kaminski, M., Holzinger, R., Wisthaler, A. and Kiendler-Scharr, A.: Comparison of three aerosol chemical characterization techniques utilizing PTR-ToF-MS: A study on freshly formed and aged biogenic SOA, *Atmos Meas Tech Discuss*, 2017, 1–31, doi:10.5194/amt-2017-288, 2017.
- 310 Gkatzelis, G. I., Tillmann, R., Hohaus, T., Müller, M., Eichler, P., Xu, K.-M., Schlag, P., Schmitt, S. H., Wegener, R., Kaminski, M., Holzinger, R., Wisthaler, A. and Kiendler-Scharr, A.: Comparison of three aerosol chemical characterization techniques utilizing PTR-ToF-MS: a study on freshly formed and aged biogenic SOA, *Atmos Meas Tech*, 11(3), 1481–1500, doi:10.5194/amt-11-1481-2018, 2018.
- 315 Grannas, A. M., Hockaday, W. C., Hatcher, P. G., Thompson, L. G. and Mosley-Thompson, E.: New revelations on the nature of organic matter in ice cores, *J. Geophys. Res. Atmospheres*, 111(D4), D04304, doi:10.1029/2005JD006251, 2006.
- Gröllert, C., Kasper, A. and Puxbaum, H.: Organic Compounds in High Alpine Snow, *Int. J. Environ. Anal. Chem.*, 67(1–4), 213–222, doi:10.1080/03067319708031405, 1997.
- 320 Guillaume, B., Liousse, C., Galy-Lacaux, C., Rosset, R., Gardrat, E., Cachier, H., Bessagnet, B. and Poisson, N.: Modeling exceptional high concentrations of carbonaceous aerosols observed at Pic du Midi in spring–summer 2003: Comparison with Sonnblick and Puy de Dôme, *Atmos. Environ.*, 42(20), 5140–5149, doi:10.1016/j.atmosenv.2008.02.024, 2008.

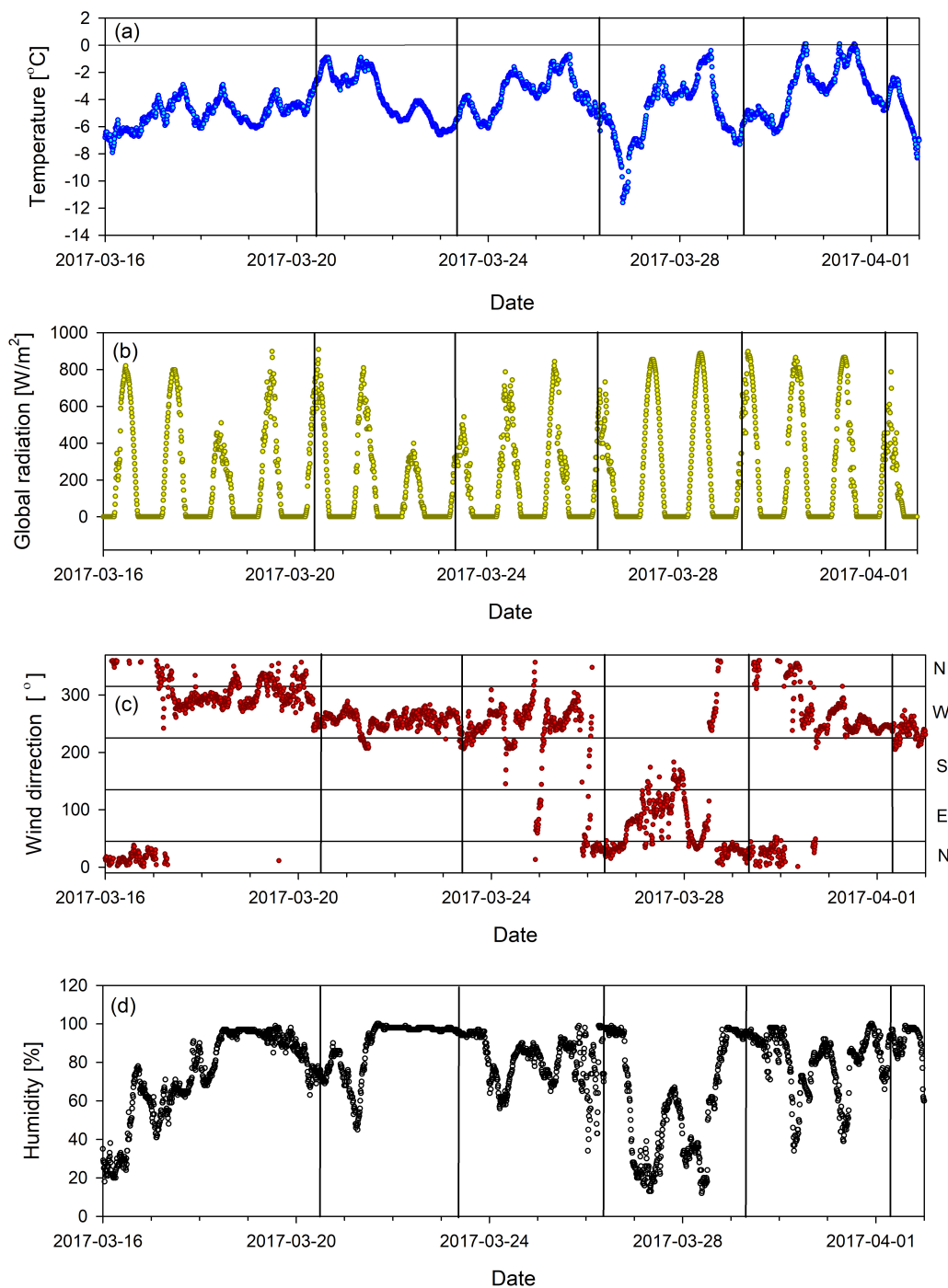


- 325 Hawkes, J. A., Dittmar, T., Patriarca, C., Tranvik, L. and Bergquist, J.: Evaluation of the Orbitrap Mass Spectrometer for the Molecular Fingerprinting Analysis of Natural Dissolved Organic Matter, *Anal. Chem.*, 88(15), 7698–7704, doi:10.1021/acs.analchem.6b01624, 2016.
- Holzinger, R.: PTRwid: A new widget tool for processing PTR-TOF-MS data, *Atmos Meas Tech*, 8(9), 3903–3922, doi:10.5194/amt-8-3903-2015, 2015.
- 330 Holzinger, R., Williams, J., Herrmann, F., Lelieveld, J., Donahue, N. M. and Röckmann, T.: Aerosol analysis using a Thermal-Desorption Proton-Transfer-Reaction Mass Spectrometer (TD-PTR-MS): a new approach to study processing of organic aerosols, *Atmos Chem Phys*, 10(5), 2257–2267, doi:10.5194/acp-10-2257-2010, 2010a.
- 335 Holzinger, R., Kasper-Giebl, A., Staudinger, M., Schauer, G. and Röckmann, T.: Analysis of the chemical composition of organic aerosol at the Mt. Sonnblick observatory using a novel high mass resolution thermal-desorption proton-transfer-reaction mass-spectrometer (hr-TD-PTR-MS), *Atmos Chem Phys*, 10(20), 10111–10128, doi:10.5194/acp-10-10111-2010, 2010b.
- Holzinger, R., Goldstein, A. H., Hayes, P. L., Jimenez, J. L. and Timkovsky, J.: Chemical evolution of organic aerosol in Los Angeles during the CalNex 2010 study, *Atmos Chem Phys*, 13(19), 10125–10141, doi:10.5194/acp-13-10125-2013, 2013.
- 340 Kroll, J. H., Donahue, N. M., Jimenez, J. L., Kessler, S. H., Canagaratna, M. R., Wilson, K. R., Altieri, K. E., Mazzoleni, L. R., Wozniak, A. S., Bluhm, H., Mysak, E. R., Smith, J. D., Kolb, C. E. and Worsnop, D. R.: Carbon oxidation state as a metric for describing the chemistry of atmospheric organic aerosol, *Nat. Chem.*, 3(2), 133–139, doi:10.1038/nchem.948, 2011.
- 345 Kujawinski, E. B., Freitas, M. A., Zang, X., Hatcher, P. G., Green-Church, K. B. and Jones, R. B.: The application of electrospray ionization mass spectrometry (ESI MS) to the structural characterization of natural organic matter, *Org. Geochem.*, 33(3), 171–180, doi:10.1016/S0146-6380(01)00149-8, 2002.
- 350 Legrand, M., Preunkert, S., Jourdain, B., Guilhermet, J., Faïn, X., Alekhina, I. and Petit, J. R.: Water-soluble organic carbon in snow and ice deposited at Alpine, Greenland, and Antarctic sites: a critical review of available data and their atmospheric relevance, *Clim Past*, 9(5), 2195–2211, doi:10.5194/cp-9-2195-2013, 2013.
- Marsh, J. J. S., Boschi, V. L., Sleighter, R. L., Grannas, A. M. and Hatcher, P. G.: Characterization of dissolved organic matter from a Greenland ice core by nanospray ionization Fourier transform ion cyclotron resonance mass spectrometry, *J. Glaciol.*, 59(214), 225–232, doi:10.3189/2013JoG12J061, 2013.
- 355 Materić, D., Bruhn, D., Turner, C., Morgan, G., Mason, N. and Gauci, V.: Methods in Plant Foliar Volatile Organic Compounds Research, *Appl. Plant Sci.*, 3(12), 1500044, doi:10.3732/apps.1500044, 2015.



- 360 Materić, D., Peacock, M., Kent, M., Cook, S., Gauci, V., Röckmann, T. and Holzinger, R.:
Characterisation of the semi-volatile component of Dissolved Organic Matter by Thermal Desorption –
Proton Transfer Reaction – Mass Spectrometry, *Sci. Rep.*, 7(1), 15936, doi:10.1038/s41598-017-16256-
x, 2017.
- 365 Müller-Tautges, C., Eichler, A., Schwikowski, M., Pezzatti, G. B., Conedera, M. and Hoffmann, T.:
Historic records of organic compounds from a high Alpine glacier: influences of biomass burning,
anthropogenic emissions, and dust transport, *Atmos Chem Phys*, 16(2), 1029–1043, doi:10.5194/acp-
16-1029-2016, 2016.
- Nguyen, T. B., Crounse, J. D., Teng, A. P., St. Clair, J. M., Paulot, F., Wolfe, G. M. and Wennberg, P.
O.: Rapid deposition of oxidized biogenic compounds to a temperate forest, *Proc. Natl. Acad. Sci. U. S.
A.*, 112(5), E392–E401, doi:10.1073/pnas.1418702112, 2015.
- 370 Pokhrel, A., Kawamura, K., Ono, K., Seki, O., Fu, P., Matoba, S. and Shiraiwa, T.: Ice core records of
monoterpene- and isoprene-SOA tracers from Aurora Peak in Alaska since 1660s: Implication for
climate change variability in the North Pacific Rim, *Atmos. Environ.*, 130(Supplement C), 105–112,
doi:10.1016/j.atmosenv.2015.09.063, 2016.
- Singh, P., Kumar, N. and Arora, M.: Degree–day factors for snow and ice for Dokriani Glacier,
Garhwal Himalayas, *J. Hydrol.*, 235(1), 1–11, doi:10.1016/S0022-1694(00)00249-3, 2000.
- 375 Strader, R., Lurmann, F. and Pandis, S. N.: Evaluation of secondary organic aerosol formation in
winter, *Atmos. Environ.*, 33(29), 4849–4863, doi:10.1016/S1352-2310(99)00310-6, 1999.
- Timkovsky, J., Dusek, U., Henzing, J. S., Kuipers, T. L., Röckmann, T. and Holzinger, R.: Offline
thermal-desorption proton-transfer-reaction mass spectrometry to study composition of organic aerosol,
J. Aerosol Sci., 79, 1–14, doi:10.1016/j.jaerosci.2014.08.010, 2015.
- 380 Zhao, Y., Hennigan, C. J., May, A. A., Tkacik, D. S., de Gouw, J. A., Gilman, J. B., Kuster, W. C.,
Borbon, A. and Robinson, A. L.: Intermediate-Volatility Organic Compounds: A Large Source of
Secondary Organic Aerosol, *Environ. Sci. Technol.*, 48(23), 13743–13750, doi:10.1021/es5035188,
2014.

385



390 **Figure 1: Meteorological data measured at Sonnblick station during the sampling: (a) temperature, (b) global radiation (c) wind direction, (d) relative humidity. Vertical lines represent the sampling time. Note the wind direction change in the period preceding the sampling at 29/03/2017**

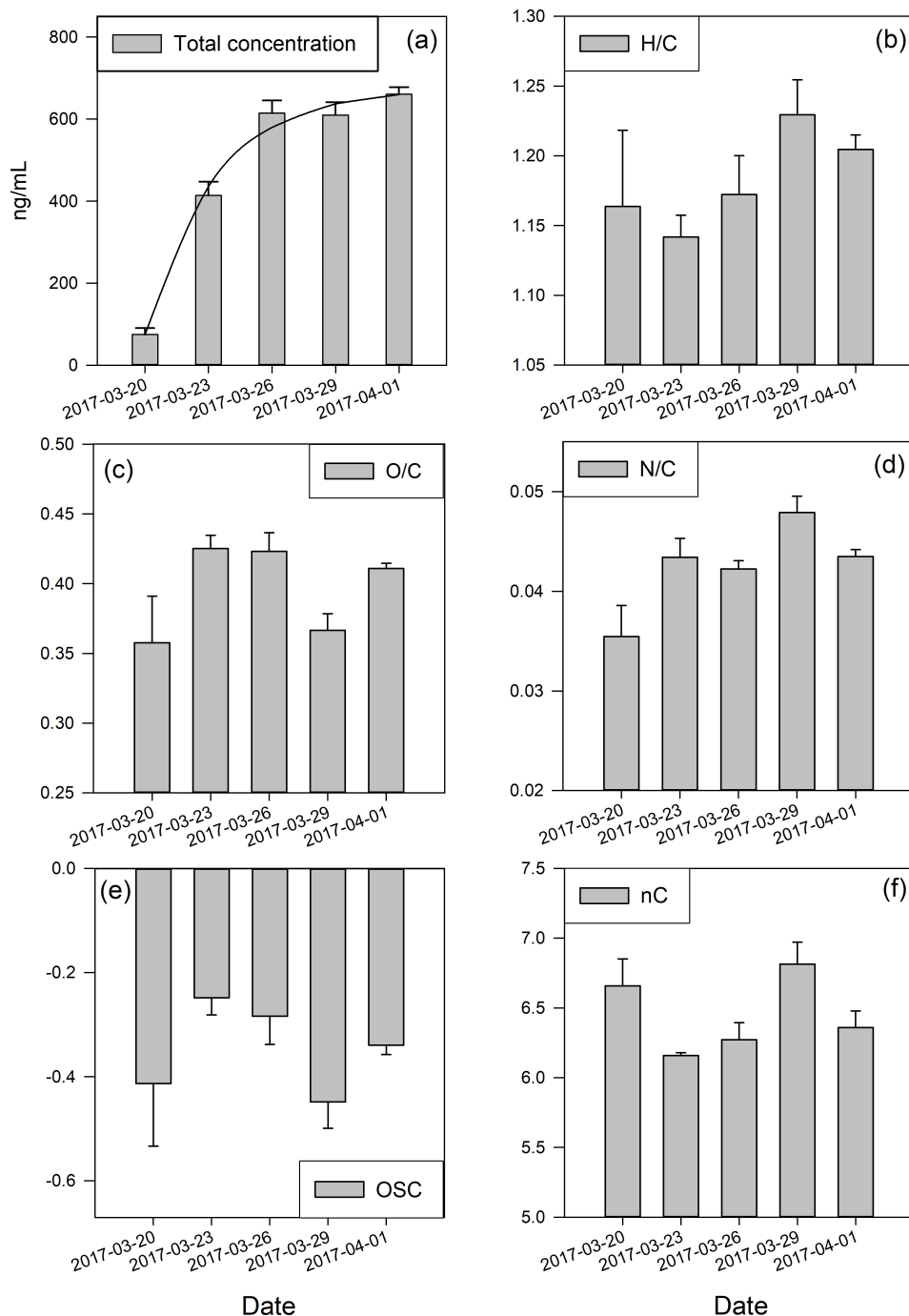
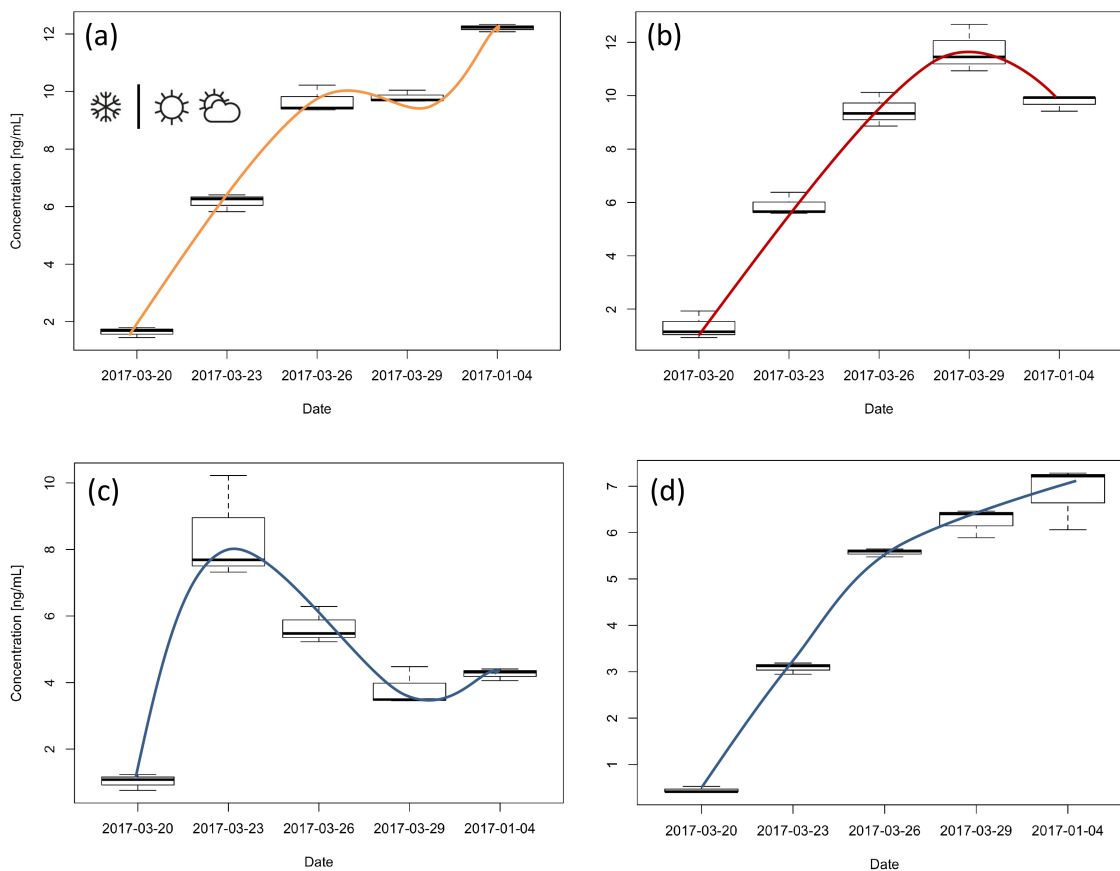


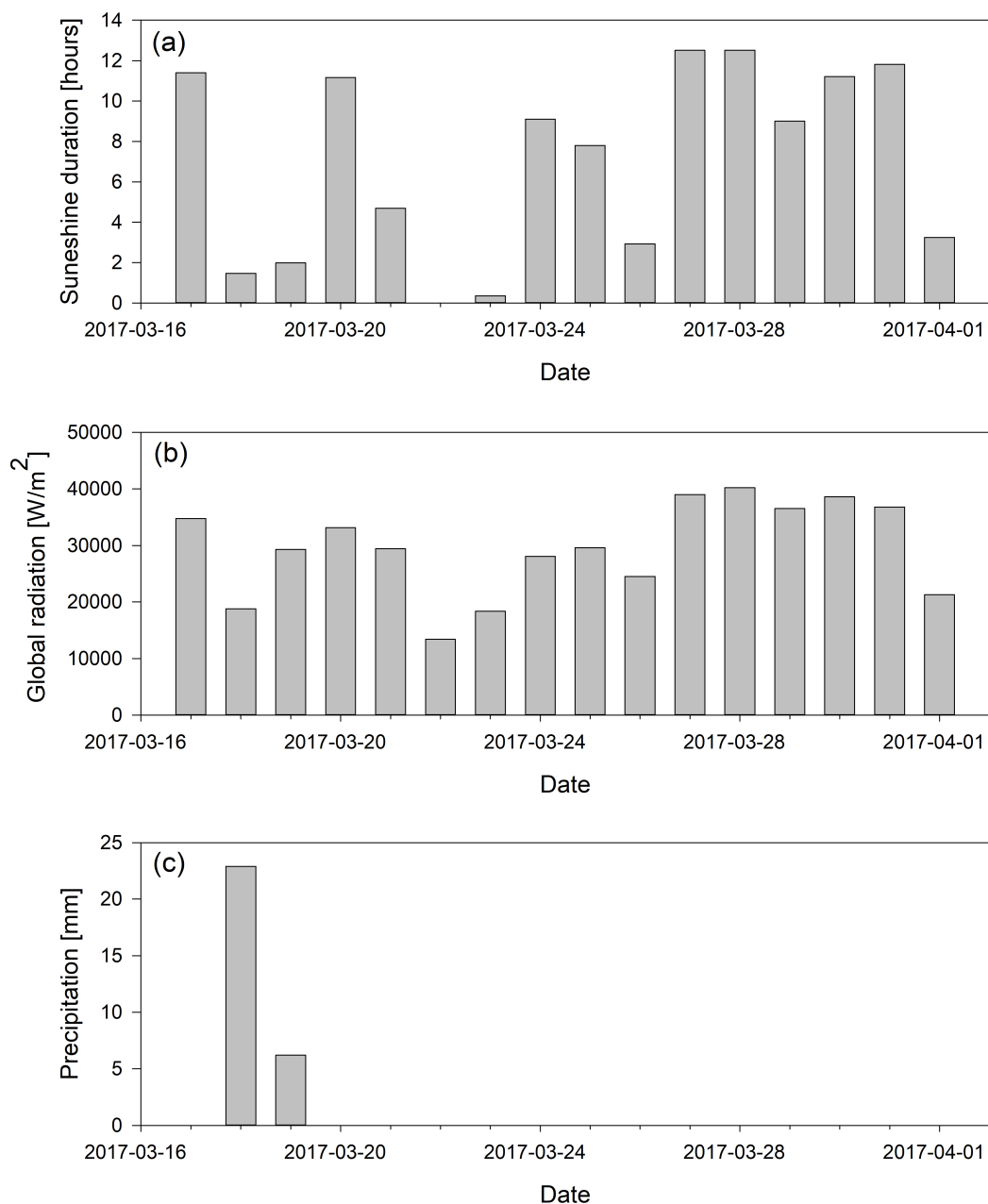
Figure 2: Total concentration of organic ions and cumulative metrics of atomic ratio distribution. (a) Total concentration in ng mL^{-1} , the line represents the fit from the simple deposition model explained in the text (Eq. 1) ;(b) H/C ratio, (c) O/C ratio, (d) N/C ratio, (e) oxidative state of carbon, (f) mean numbers of carbon. The error bars represent the standard deviation of three replicates.



400 **Figure 3: Boxplots of concentration for ions representing four distinctive groups: (a) ion m/z 115.070 - pinonic acid, (b) ion m/z 85.029 - levoglucosan, (c) ions m/z 99.008 and (d) ion m/z 159.065. The lines illustrate the change in the concentration over the time that is typical for each group.**



5. Appendices



405 **Figure A1: Light conditions and precipitation during the sampling period. (a) Global radiation [W m^{-2}] integrated for each day, (b) total daily sunshine duration in hours, (c) precipitation for the sampling period.**



410 **Table A1: Groups of ions as identified using linear regression model. Note that different thresholds of R^2 values are used to isolate the groups.**

Pinonic acid		Levogluconan		Increasing and saturating		Decreasing	
m/z	R^2	m/z	R^2	m/z	R^2	m/z	R^2
56.047	0.9828	28.017	0.9338	139.069	0.9953	80.039	0.7119
60.045	0.9823	31.018	0.9418	141.057	0.9955	99.008	1.0000
115.070	1.0000	45.033	0.9951	153.087	0.9980	113.029	0.9236
129.055	0.9810	53.038	0.9080	155.073	0.9963	140.040	0.7492
131.104	0.9918	68.052	0.9031	157.065	0.9988	163.050	0.9373
143.069	0.9919	69.034	0.9279	158.069	0.9968	192.057	0.9494
144.069	0.9877	70.033	0.9625	159.065	1.0000	193.055	0.9494
160.068	0.9832	70.068	0.9068	168.091	0.9974	194.050	0.8473
172.076	0.9813	72.046	0.9092	169.087	0.9970	357.071	0.9773
185.096	0.9871	73.028	0.9307	170.085	0.9964		
186.091	0.9865	74.029	0.9523	171.076	0.9994		
195.104	0.9800	75.043	0.9230	173.078	0.9958		
197.100	0.9806	78.994	0.9877	174.078	0.9967		
200.095	0.9801	82.036	0.9032	183.098	0.9954		
202.092	0.9824	84.046	0.9548	184.100	0.9997		
211.116	0.9948	85.029	0.9265	199.098	0.9955		
213.104	0.9819	86.027	0.9307	209.127	0.9966		
214.097	0.9803	86.060	0.9290	227.127	0.9986		
218.086	0.9861	91.040	0.9349	235.152	0.9999		
228.107	0.9943	94.038	0.9260	239.131	0.9951		
230.096	0.9816	97.029	1.0000	244.095	0.9952		
237.132	0.9828	97.060	0.9201				
246.106	0.9845	100.040	0.9043				
259.098	0.9821	108.050	0.9351				
299.065	0.9882	109.061	0.9129				
	0.9876	112.042	0.9003				
	0.9864	126.057	0.9111				
	0.9906	190.966	0.9696				
	0.9946	226.119	0.9447				
	0.9907	257.248	0.9258				
	0.9818	275.263	0.9426				
	0.9819	284.267	0.9529				
		341.339	0.9064				